Immunosensor application based on Raman spectroscopy of porous silicon

Tao Jiang (江 涛)[1], Jiaqing Mo (莫家庆)[2], Xiaoyi Lü (吕小毅)[2], Pengfei Yan (晏鹏飞)[3], Zhenhong Jia (贾振红)[4*], Jiangwei Li (李江伟)[3], and Fuchun Zhang (张富春)[3]

[1]*School of Physics, Xinjiang University, Urumqi 830046, China*

[2]*School of Electronic and Information Engineering, Xi'an Jiaotong University, Xi'an 710049, China*

[3]*Key Laboratory of Xinjiang Biological Resources and Gene Engineering, College of Life Sciences and Technology, Xinjiang University, Urumqi 830046, China*

[4]*College of Information Science and Engineering, Xinjiang University, Urumqi 830046, China*

[*]*Corresponding author: jzhh@xju.edu.cn*

Received June 29, 2010; accepted October 14, 2010; posted online January 28, 2011

Porous silicon (PS) suitable for optical detection of immunoreaction is fabricated. The structure of immunosensor is prepared by the following steps: oxidization, silanization, glutaraldehyde cross-linker, and covalent binding of antibody. When antigen is added into the immunosensor, the Raman intensity is estimated to be linearly reduced according to the concentration of the surface protective antigen protein A (spaA) of below 4.0 μg·ml^{-1}. The ultimate detection limit is 1.412×10^2 pg·ml^{-1}. Controlled experiments are also presented with non-immune antigen of the spaA, and results show that the immunosensor has high specificity. Compared with the conventional enzyme-linked immuno sorbent assay (ELISA), this method is quick, inexpensive, and label-free.

OCIS codes: 280.1415, 070.0070, 070.4790, 280.0280.

doi: 10.3788/COL201109.022801.

Various optical detection applications based on porous silicon (PS) have attracted great attention due to their remarkable optical properties and large functional surface area[1,2]. The specific surface morphology of PS makes it suitable for many different applications in various fields[3], including biosensing and optical detection of biomolecules[4−6]. Moreover, the optical behavior of PS is extremely sensitive due to its large specific surface area[7,8]. Over the past decade, more and more studies on immunosensor applications based on PS have been reported in top international academic publications[9,10]. Raman spectroscopy, particularly with near-infrared laser excitation to avoid fluorescence, has been applied successfully to extract significant biochemical information. Thus, Raman spectroscopy can be an effective and sensitive tool for monitoring the specific interactions between antibodies and antigens. However, there has been no report on immunosensor applications based on Fourier transform (FT) Raman spectroscopy of PS.

Erysipelothrix rhusiopathiae is a bacterium that causes erysipelas in swine and a variety of diseases in other animals, such as erysipeloid, which is a type of human skin disease. The surface protective antigen protein A (spaA) of erysipelothrix rhusiopathiae has been shown to be highly immunogenic, and is a potential candidate for vaccine against erysipelas[11,12]. Therefore, the rapid and accurate determination of the concentration of the spaA of erysipelothrix rhusiopathiae plays a significant role in preventing and monitoring erysipelas in swine and a variety of diseases in other animals. Success in this endeavor would be helpful for food safety and the human health.

Based on the principle that PS Raman intensity changes after spaA immobilization, we have developed a novel and rapid-detection immunosensor. This immunosensor has many advantages, such as being label-free and inexpensive, and having high sensitivity compared with the conventional enzyme-linked immuno sorbent assay (ELISA).

PS substrates were fabricated from polished N-type (100) monocrystalline silicon wafers (resistivity of 0.01–0.02 Ω·cm) using double-cell electrochemical etching method in HF/ethanol (1:4) solution. The electrolyte process was automatically and accurately controlled by a computer at current density of 55 mA/cm^2 for 150 s. After the formation of porous layers, the chips were rinsed in deionized water and ethanol, and subsequently blow-dried with nitrogen[13].

After electrochemical etching, the fresh PS surface is predominately hydride-terminated, which is slowly oxidized in the air, indicating that the optical properties of PS are unstable. In order to increase the characteristic stability of PS, the surface of PS must be oxidized by hydrogen peroxide. Furthermore, the oxidization provides the silanization required for the –OH bond. In this experiment, the substrates were immersed into H_2O_2 (30%) for 3 h at 55 °C, then subsequently dried with nitrogen.

The process of biofunctionalization and covalent binding of antibody (shown in Fig. 1) comprised the following steps:

1) The PS substrates were immersed into 5% solution of 3-aminopropyltriethoxysilane (APTES) in water/ethanol mixture (1:1) for 3 h, then thoroughly rinsed with ethanol and deionized water. The samples were dried with nitrogen and baked in an oven at 100 °C for 10 min.

2) After silanization, the samples were immersed into a solution of glutaraldehyde (3%) in phosphate buffer silane (PBS, pH = 7.4) at 25 °C for 50 min. The samples

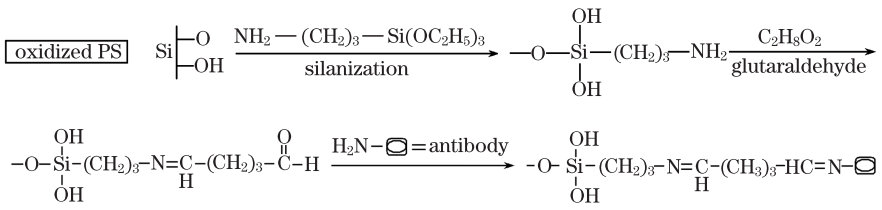

Fig. 1. Biofunctionalization process of PS and covalent binding of antibody.

were then rinsed with water in order to remove all the excess glutaraldehyde.

3) The spaA immune antibody was dropped onto the treated samples at 37 °C for 3 h. Likewise, 30 μl of spaA non-immunity antibody was dropped onto the treated samples at 37 °C for 2 h. All samples were then thoroughly cleaned with PBS and water. Finally, in order to prevent nonspecific adsorption, the substrates were dipped into a 0.1% bovine serum albumin (BSA) solution at room temperature for 30 min.

After briefly rinsing with deionized water, all the substrates were immersed into different concentrations of spaA at 37 °C for 2 h. Then, the PS films were rinsed thoroughly with PBS and deionized water. Antibodies and antigen were prepared in the Key Laboratory of Xinjiang Biological Resources and Gene Engineering, College of Life Sciences and Technology, Xinjiang University, and were kept frozen until use.

The Raman spectra of all the samples were recorded using VERTEX 70-RAM II FT-Raman spectrometer (Bruker Company, Germany) under the same conditions (excitation wavelength of 1064 nm, laser power of 3 mW, and temperature of 25 °C).

The surface of the fresh PS was observed using scanning electron microscope (SEM), as shown in Fig. 2(a). The average pore dimension is approximately 310 nm. In this experiment, the diameter of the biomolecules is less than 50 nm, making their immobilization into pores of PS easy.

In addition, when excited by ultraviolet (UV) light with wavelength of 370 nm, the PS emits bright fluorescence at 581 nm, as shown in Fig. 2(b). The porosity of the samples is determined to be 81% through the gravimetric method. Hence, for sensor applications, the substrates provide a large and often highly reactive surface area, which effectively captures and detects molecules in large quantities.

The stability of the samples was studied by measuring the reduction in Raman intensity of the same chip every 5 d. The PS films remain stable for more than a month,

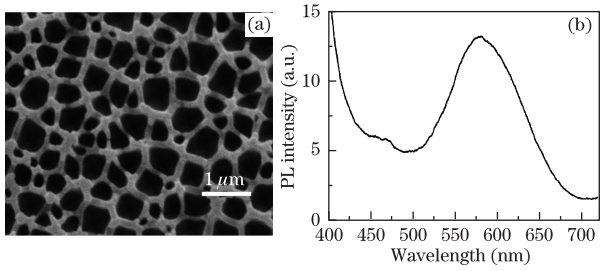

Fig. 2. (a) Top view of SEM image of PS formed in 55 mA/cm^2 for 120 s; (b) PL intensity of PS. PL: photolumine scence.

as shown in Fig. 3 (additional data not shown). After being oxidized with H_2O_2, the PS surface was modified with Si–OH and Si–O, causing it to become stable and ready for immunosensor application.

Diffuse absorbance FT-infrared (IR) spectroscopy was used to monitor the functionalization reactions of the PS. As shown in Fig. 4, after functionalization of the surface with APTES, the silanized wafers exhibit two small bands at 1602 cm^{-1} and near 3310 cm^{-1}, which are attributed to –NH bonds[14,15]. Another small band, at 2937 cm^{-1}, can be attributed to –CH bonds. Glutaraldehyde-activated samples do not show any bands corresponding to –NH bonds. The distinct bands at 1580 cm^{-1} (imine –C=N) and 1710 cm^{-1} (–C=O of aldehyde) correspond to glutaraldehyde-activated sample, denoting that the functionalization of the PS is successful in immobilizing biomolecules.

To demonstrate specificity, Fig. 5(a) shows the Raman intensity of samples with immune antibody after being immersed into the spaA. A reduction in Raman intensity was detected, which can be attributed to the specific antigen-antibody reaction on the surface of PS. For samples with non-immune antibody, negligible reduction in Raman intensity was detected after being immersed into the spaA (Fig. 5(b)), which indicated that there was specific absorption of spaA inside the pores of PS.

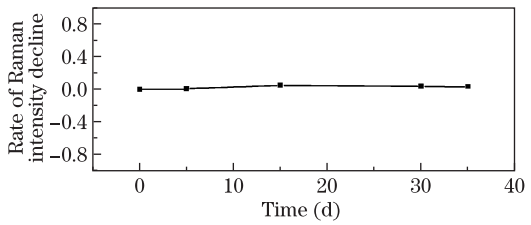

Fig. 3. Intensity of PS Raman stability for more than a month.

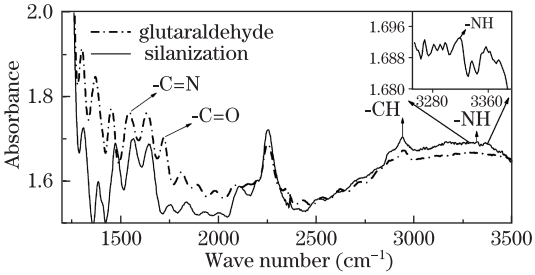

Fig. 4. FT-IR absorbance spectra of PS after silanization and treatment with glutaraldehyde.

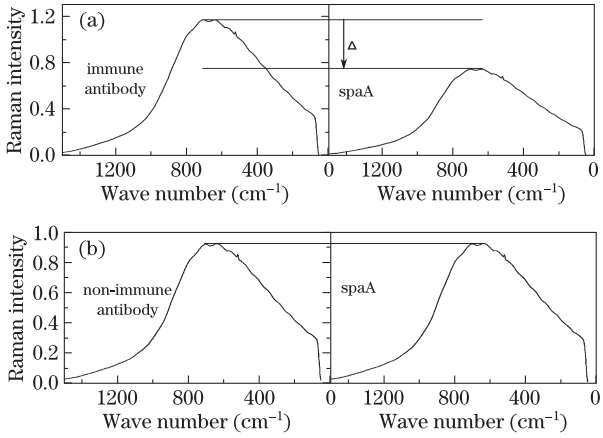

Fig. 5. Representing PS substrates can distinguish immune and non-immune antibodies of erysipelothrix rhusiopathiae. Raman intensity of PS with (a) immune antibody was reduced after being immersed into the spaA (10 μg·ml^{-1}) and (b) non-immune antibody was negligibly reduced after being immersed into the spaA (10 μg·ml^{-1}).

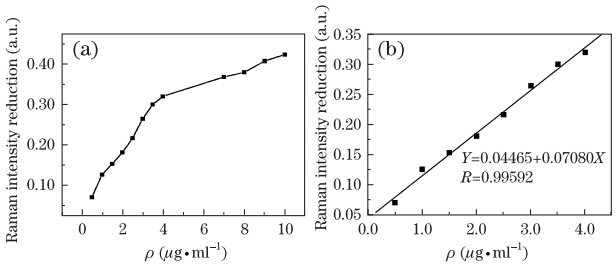

Fig. 6. Raman intensity reduction after the immersion of samples into different concentrations of spaA. (a) ρ = 0–10 μg·ml^{-1}; (b) ρ = 0–4.0 μg·ml^{-1}.

The reduction in Raman intensity is shown in Fig. 6(a). This reduction was determined by immersing the PS wafers (after BSA blocking) into different spaA concentrations. The Raman intensity decreased proportionally to the concentration ρ of spaA (lower than 10 μg·ml^{-1}). When the spaA concentration was greater than 10 μg·ml^{-1}, the reduction in Raman intensity became much less, indicating that the surfaces of the chips have become saturated with SpaA, as shown in Fig. 6(a). The linear fit of the experimental data in Fig. 6(b) provides the sensitivity of the sensor, which is at 0.0708 a.u./(μg·ml^{-1}). Given that the Raman intensity resolution of the FT-Raman spectrometer is 0.00001 a.u., the ultimate detection limit of the PS immunosensor is ρ= 0.00001 a.u./(0.0708 a.u./(μg·ml^{-1})) = 1.412 × 10^2 pg·ml^{-1}[16]. All the experiments in this letter were undertaken in triplicate, and the obtained results were compared.

The reduction in Raman intensity is presumably caused by the antigen-antibody reaction on PS. The thickness, pore size, and surface chemistry of PS are all subject to change. Furthermore, the Raman intensity is likely absorbed by the biomolecules, and is thereby reduced.

In conclusion, PS chips are used for monitoring antibody-antigen interaction. Raman spectroscopy provides a sensitive tool for monitoring the specific interaction between antibody and antigen. The stability and advantages of the immunosensor are discussed. The results demonstrate the successful detection of spaA by the changes in Raman spectrum. The reduction in the Raman intensity is estimated to be linearly related to the concentration of the spaA of below 4.0 μg·ml^{-1}, with the ultimate detection limit being approximately 1.412 × 10^2 pg·ml^{-1}. Compared with ELISA, PS immunosensor is quick, specific, inexpensive, and label-free. As a measurement system, it is simple to operate and offers high specificity. The experimental results can pave the way for the development of PS immunosensor based on the change in Raman intensity. The advantages of this PS immunosensor can be applied in practice in many fields.

This work was supported by the National Natural Science Foundation of China (No. 60968002) and the Program for New Century Excellent Talents in University of China (NCET-05-0897).

References

1. G. de Cesare, G. Maiello, G. Masini, V. Bondarenko, and A. Ferrari, J. Non-Cryst. Solids **227-230,** 1354 (1998).
2. J. Zhang, W. Zhang, S. Dong, A. P. F. Turner, Q. Fan, and S. Jia, Anal. Lett. **40,** 1549 (2007).
3. X. Lü, J. Hou, M. Xiang, Z. Jia, and F. Zhong, Chin. Opt. Lett. **8,** 618 (2010).
4. K.-P. S. Dancil, D. P. Greiner, and M. J. Sailor, J. Am. Chem. Soc. **121,** 7925 (1999).
5. R. R. K. Reddy, A. Chadha, and E. Bhattacharya, Biosens. Bioelectron. **16,** 313 (2001).
6. J. Chapron, A. Alekseev, V. Lysenko, V. N. Zaitsev, and D. Barbier, Sens. Actuat. B. **12,** 706 (2007).
7. A. M. Rossi, L. Wang, V. Reipa, and T. E. Murphy, Biosens. Bioelectron. **23,** 741 (2007).
8. J. López-García, R. J. Martín-Palma, M. Manso, and J. M. Martínez-Duart, Sens. Actuat. B **126,**82 (2007).
9. J. Yakovlevaa, R. Davidsson, M. Bengtsson, T. Laurell, and J. Emnéusb, Biosens. Bioelectron. **19,** 21 (2003).
10. O. Meskini, A. Abdelghani, A. Tlili, R. Mgaieth, N. Jaffrezic-Renault, and C. Martelet, Talanta **71,** 1430 (2007).
11. G. Zhang, H. To, K. E. Russell, L. R. Hendrix, T. Yamaguchi, H. Fukushi, K. Hirai, and J. E. Samuel, Infect. Immun. **73,** 1561 (2005).
12. H. To and S. Nagai, Clin. Vaccine. Immunol. **14,** 813 (2007).
13. H. Ouyang, M. Christophersen, R. Viard, B. L. Miller, and P. M. Fauchet, Adv. Funct. Mater. **15,** 1851 (2005).
14. C. A. Canaria, I. N. Lees, A. W. Wun, G. M. Miskelly, and M. J. Sailor, Inorg. Chem. Commun. **5,** 560 (2002).
15. R. E. Fernandeza, E. Bhattacharya, and A. Chadha, Appl. Surf. Sci. **254,** 4512 (2008).
16. G. Rong, J. D. Ryckman, R. L. Mernaugh, and S. M. Weiss, Appl. Phys. Lett. **93,** 161109 (2008).